



Article

Monitoring of Stator Winding Insulation Degradation through Estimation of Stator Winding Temperature and Leakage Current

Laszlo Szamel  and Jackson Oloo * 

Department of Electric Power Engineering, Budapest University of Technology and Economics, Egry József Utca 18, H-1111 Budapest, Hungary; szamel.laszlo@vik.bme.hu

* Correspondence: joloo@edu.bme.hu

Abstract: Switched Reluctance Motors (SRMs), Permanent Magnet Synchronous Motors (PMSMs), and induction motors may experience failures due to insulation-related breakdowns. The SRM rotor is of a non-salient nature and made of solid steel material. There are no windings on the rotor. However, the stator is composed of windings that are intricately insulated from each other using materials such as enamel wire, polymer films, mica tapes, epoxy resin, varnishes, or insulating tapes. The dielectric strength of the insulation may fail over time due to several environmental factors and processes. Dielectric breakdown of the winding insulation can be caused by rapid switching of the winding current, the presence of contaminants, and thermal aging. For reliable and efficient operation of the SRMs and other electrical machines, it is necessary to take into account the physics of the winding insulation and perform appropriate diagnostics and estimations that can monitor the integrity of the insulation. This article presents the estimation problem using a Genetic Algorithm (GA)-optimized Random Forest Regressor. Empirical properties and measurable quantities in the historical data are utilized to derive temperature and leakage current estimation. The developed model is then combined with a moving average function to increase the accuracy of prediction of the stator winding temperature and leakage current. The performance of the model is compared with that of the Feedforward Neural Network and Long Short-Term Memory over the same winding temperature and leakage current historical data. The performance metrics are based on computation of the Mean Square Error and Mean Absolute Error.



Citation: Szamel, L.; Oloo, J. Monitoring of Stator Winding Insulation Degradation through Estimation of Stator Winding Temperature and Leakage Current. *Machines* **2024**, *12*, 220. <https://doi.org/10.3390/machines12040220>

Academic Editors: Giacomo Scelba and Luigi Danilo Tornello

Received: 28 February 2024

Revised: 22 March 2024

Accepted: 23 March 2024

Published: 26 March 2024



Copyright: © 2024 by the authors. Licensee MDPI, Basel, Switzerland. This article is an open access article distributed under the terms and conditions of the Creative Commons Attribution (CC BY) license (<https://creativecommons.org/licenses/by/4.0/>).

Keywords: insulation degradation; machine learning; random forest regression; genetic algorithm; predictive maintenance; stator windings

1. Introduction

In electrical machines, effective winding insulation ensures electrical isolation by preventing conduction in neighboring motor windings. Separation between phases also ensures protection against short circuits. Optimal operating temperatures within the motor can also be maintained through a thermal barrier provided by the insulation material. Lastly, physical damage to the winding is reduced through structural support provided by the insulation material. The general approach to the system of winding insulation in motors involves the multi-layered arrangement of coils and slots [1]. The insulation thickness is considered such that the design margin has an integrity against breakdown that is much higher than the allowed voltage.

For electrical machines, there are three regions that can be pointed out along the winding lengths, namely, slot area (coils sides), and end winding and end extension areas. The dielectric properties of the winding insulation deteriorate gradually as a result of air gaps in the slot area. Discharges may occur in the portions with the presence of an air layer during voltage stresses. Over time, gradual electric erosion leads to reduced dielectric strength of the winding insulation, eventually leading to breakdown [1–3]. Additionally, the presence of air gaps in the insulation encourages dust penetration, which, especially

in an area with carbon and metals, becomes conductive. To solve the problems of voids occurring in the insulation material, researchers have come up with novel methods of administering insulation such as the vacuum pressure impregnation of varnish and epoxy resin. Stator winding insulation aging is accelerated by the following factors:

(i) Contamination

SRMs, as an alternative for the automotive industry, are bound to be used in different random environments. Exposure to harsh environments such as saline contamination, chemical impurities, dust, moisture, vibrations, oil penetration, radiation exposure, high pressure, and ambient humidity may lead to potential discharges by making the surface of the insulators conductive. SRMs are also applicable to agriculture, industry, and the needs around coastal regions, which may lead to contamination of insulator surfaces. The contaminant layers deposited over the insulator surfaces may not be conductive when dry, but the conductivity increases with the presence of a light amount of moisture to form an electrolyte. A progressive increase in conductivity results in more frequent and increasing intensity of partial discharges, which may damage the insulator surface [3].

(ii) Voltage stress

The converter switching for activation of proper phase windings during SRM operation introduces voltage spikes due to high-speed switching. As a result, corona, partial discharges, and even insulation breakdown may occur in cases where the insulation is in the process of degradation. Rapid switching of stator currents in the phase windings leads to high electrical exposure of the insulation during the transient states. In some cases, even at rated voltages, exposure to an electric field leads to ionization of the layered system gases. The layered system gaps hence develop localized partial discharges with the formation of nitrogen oxide and ozone [4]. Partial discharges over a long time have been observed to expose the insulating material to deep erosion, thereby compromising its dielectric strength. Insulating materials such as pressboards, papers, and oil cloths should be avoided as they have low resistance toward partial discharges. Mica provides the best resistance to partial discharge [5].

(iii) Thermal stress

Over time, the dielectric strength of the winding insulation material may reduce due to the accelerated aging of insulation material. Aging of the insulation material may be aided by high operating temperatures outside and within the motor [6]. Due to unfavorable working conditions, permanent damage may be incurred in the structure of the insulation material. The insulation structural properties affected include permittivity, dielectric strength, dielectric loss, and mechanical strength due to evaporation of the varnish. It is therefore imperative that the motor operating temperature is monitored for the preservation of insulation integrity. This paper uses empirical data on stator winding temperatures to create a prediction model for temperature estimation over time. In view of this, it is possible to plan for the preventive maintenance of motor insulation.

2. Diagnostic Mechanisms of Winding Insulation Health and Monitoring

It is important to track the integrity of insulators in electrical machines to prevent unexpected breakdowns over time. Three important aspects of insulation diagnostics are DC polarization, loss of the insulation system, and partial discharge. The diagnostic criteria allow for a prediction of the duration of reliability of the motor. It also allows for repair and maintenance planning of the machine. The commonly used diagnostic techniques are as follows:

2.1. Insulation Resistance Test

Measurement of the SRM winding insulation integrity, also known as the ground wall, can be accomplished through an insulation resistance test. Here, the motor frame is used as a ground reference while the DC voltage is applied across the motor leads. The applied

voltage is sustained for over 60 s so that the leakage current from the winding insulations can be measured. The megohmmeter, the instrument used for the measurement, gives the insulation resistance as calculated from the sustained leakage current. Table 1 gives the IEEE 43 guideline standards for the application of IR tests with regard to voltage ratings [7].

Table 1. IR test voltage rating guidelines in relation to winding voltages.

Rated Voltage (V)	Insulation Resistance Test Voltage (V)
<1000	500
1000–2500	500–1000
2501–5000	1000–2500
5001–12,000	2500–5000
>12,000	5000–10,000

The insulation integrity is classified in Table 2 with regard to the insulation resistance value.

Table 2. Classification of insulation integrity.

Value of Insulation Resistance	Level of Insulation
Less than 2 MΩ	Bad
2–5 MΩ	Critical
5–10 MΩ	Abnormal
10–50 MΩ	Good
50–100 MΩ	Very good
More than 100 MΩ	Excellent

This paper uses empirical data on winding leakage current for different test runs to predict insulation degradation over time by applying different machine learning techniques for leakage current estimation in a time series forecast.

2.2. Insulation Thermal Imaging

Generally, motor winding insulations are based on classes. The National Electrical Manufacturers Association (NEMA) dictates operating temperatures for every insulation class, as shown in Table 3 [8,9]. These allowable temperatures are based on a full-load operation.

Table 3. Temperature rating for motor winding insulation.

Class	Temperature Rating	Ambient Temperature	Hotspots
A	105	+40	+5
B	130	+40	+10
F	155	+40	+10
H	180	+40	+15

The insulation classes are categorized according to the polarization index, PI , which is the ratio of insulation resistance measurement after 10 min, as is shown in Equation (1), [9].

$$PI = \frac{R_{600}}{R_{60}} \quad (1)$$

where R_{600} and R_{60} are the insulation resistance values after 600 min and 60 min, respectively. The recommended values of the PI are as shown in Table 4 [9,10].

Table 4. Polarization Index for classification of insulation condition.

PI	The Insulation Condition
1.0–2.0	Incorrect
2.0–4.0	Good
>4.0	Very good

The categorization of insulation classes is shown in Table 5 [9,10].

Table 5. Polarization Index categorization of insulation classes.

PI	Insulation Class
1.5	A
2.0	B
2.0	F
2.0	H

Infrared cameras can be used to scan for winding hotspots due to temperature variations within the motor. Additionally, infrared thermography was applied to a non-destructive test to detect temperature variations on the surface of the motor. Hotspots on the windings are an indication of insulation degradation. SRM nameplates have a normal operating temperature indicated on them. The exterior motor temperature increases with an increase in internal temperature. It has been found that a winding temperature increase of 10 °C above the rated nameplate temperature degrades the life of winding insulators by approximately 50 percent. Since the infrared camera does not access the internal operating temperatures of the motor, the motor surface temperature is captured by the infrared camera. Therefore, for temperature readings from the middle of the motor frame, abnormally high temperature sources within the motor, i.e., coupling, windings, and bearings, can be easily pointed out from an infrared image. Ref. [11] uses an infrared thermograph for inspection and then applies deep learning-based hotspot localization based on segmentation of the motor windings. Smith et al. [12] present an experimental study on novel insulation wire materials for stator winding designs that can withstand high temperatures. Various materials were tested for temperature dependency performance, including a MAGNETEMP CA-200 wire, standard Class H enamel wire, CERAFIL 500 wire, VonRoll SK650 wire, S-2 glass fiber, and Photonis glass-coated wire. The materials were investigated, as prospective winding material wires, for insulation systems operating in an over 375 °C thermal environment.

This paper uses empirical data on stator winding temperature for different test runs to predict insulation degradation over time by applying different machine learning techniques for leakage current estimation in a time series forecast.

2.3. Partial Discharge Test

Most converter-powered electric motors experience voltage stress due to the rapid switching of currents in the windings. These short operating times of phase windings result in latent defects that are only detectable through partial discharge measurements. Sometimes the applied voltage may not be able to break down the insulation material and the fault may go unnoticed over a period of time. Performing an AC dielectric strength test simultaneously with a partial discharge test can identify and filter out the insulation defects. On mitigating partial discharge in motor windings, [13] adds a thin layer of conducting material on the surface of the enamel wire used in constructing the motor winding. The

objective is to localize the PD occurrences to avoid random instances that would otherwise have been experienced in the residual voids. The PD activity is highly reduced through the addition of varnish in small quantities in the ascertained critical zones.

2.4. Online and Offline Monitoring

Sensors can be used to provide online monitoring of insulation conditions by measuring physical quantities such as magnetic flux, stator current, and motor internal temperature. Offline, historical data from the sensors can be used to perform time series forecasting of the behavior of factors influencing the health of the insulation materials. Predictive maintenance of the motor windings relies on diagnostic techniques to ascertain when significant aging of the insulation of material has occurred and, thus, help in planning for avoidance of failure during service. Online monitoring and offline diagnostics such as partial discharge, magnetic flux, end winding vibration, and temperature have been well explored by researchers over the years. New methods such as dielectric spectroscopy, polarization current, and online leakage current monitoring are currently being introduced. However, the monitoring of stator winding temperature and leakage currents requires efficient sensors, which may occasionally fail. It is for these reasons that there is a need to utilize historical data from the sensors to estimate future trends of the physical quantities that point toward the aging of insulation material.

2.5. Prediction of Stator Winding Temperature

For air-cooled machines, thermal stress has been the major cause of insulation deterioration. Thermal stress accelerates the breakdown of chains between molecules into smaller ones in the process of insulation aging. Insulation delamination is also caused by overheating. Therefore, the main purpose of monitoring the stator winding temperature is to ensure insulation integrity, which ensures the mitigation of future damage resulting from inter-turn faults. Insulation aging caused by inter-turn short-circuit faults results in high winding temperatures. Moreover, hotspots around the insulation accelerate aging due to higher localized temperatures.

Thermocouples are the main devices utilized in temperature measurement of the stator windings. However, such devices only provide an alarm notification for abnormal temperature values during operation. These sensors may also suffer false-positive and false-negative phenomena. Therefore, there is a need to use historical data to estimate and predict future temperature trends even when the sensors have long failed. Temperature analysis of the SRM in relation to insulation integrity has not been extensively studied. The service life of winding insulations critically depends on the internal motor temperatures and the ambient temperature. *Copper losses*, *core losses*, and *friction losses* are the common sources of temperature rise within the motor. Stator copper losses are a major contributor to temperature variations within the motor, even though the lack of rotor windings contributes to temperature rise limitations. Moreover, the alternating electric field leads to dielectric polarization and incomplete discharges. The discharges result in rising local temperatures. The internal heat due to high internal temperatures is given in Equation (2) [14].

$$H_g = \frac{\text{Copper Losses (W)}}{\text{Coil Volume (m}^3\text{)}} \quad (2)$$

The stator coils are the source of copper losses. The *copper losses* are defined in Equation (3) [15].

$$P_{cu} = R_p I_p^2 \quad (3)$$

In switched reluctance machines, the core losses were determined experimentally from [16] as:

$$P_{core} = a f^b \left(\frac{V}{f}\right)^c \quad (4)$$

where a , b , and c are constants, and f is the second mode natural frequency.

The viscous flow experienced over the rotor, and the relative motion of the bearings, presents friction losses given in Equation (5) [16].

$$P_{fric} = a \cdot rpm + b \cdot rpm^2 \quad (5)$$

The above losses are shared in different sections of the motor as heat flow sources.

Recently, researchers have performed a thermal field analysis of switched reluctance motors for reliable and safe operation. However, the vulnerability of SRM drives due to insulation degradation faults needs attention. It is therefore imperative to develop intelligent methods of insulation health monitoring and diagnosis. Motor surface temperatures have easily been monitored using sensors mounted near the couplings. However, internal temperatures, which generally affect the integrity of the insulation, have been a challenge for a number of reasons. The performance of temperature sensors inside the motors is easily affected by the heat from the copper losses, resulting in sensor faults. The thermal problem can be easily solved by the introduction of sufficient and adequate ventilation during motor design and manufacture. However, the introduction of ventilation would require more space and, therefore, an increase in costs. Consequently, it is critical to developing intelligent methods of insulation health monitoring and diagnosis based on the time series forecasting of temperature behavior within and around the stator windings. This paper considers low-voltage stator windings of below 700 V. For windings of these voltage levels, inter-turn shorts rapidly develop into phase-to-phase shorts. This kind of insulator failure can be very rapid as compared to high-voltage stator winding insulation breakdown. Therefore, there is a need for inter-turn short-circuit diagnosis due to insulation degradation as this will provide an early warning of low-voltage stator insulation faults.

According to [17], stator winding insulation faults account for 20% to 39% of overall motor faults, and one of the most prominent causes of insulation failure is the rising temperature over time. Online and offline analysis of the temperature trend is therefore necessary. Online monitoring enables identification of faults in the initial phases and, therefore, preventive actions can be planned to alleviate critical downtimes of the machine. However, online monitoring can face challenges such as sensor faults and the increased cost of sensor installations. Although offline techniques investigated in this paper depend on historical data, they are non-invasive and operate on anomaly detection within the data. Temperature monitoring methods can also be categorized into contact direct measurement techniques, such as infrared and contactless estimation methods. The applicability of contact-based methods is limited by the need for accessibility within the mechanical structure of the motor, thereby increasing the cost of manufacturing. On the other hand, sensorless estimation methods use temperature derivations based on intelligence algorithms. Refs. [18,19] present models and iterative algorithms with measurable quantities to estimate temperature values for a permanent magnet synchronous motor. However, from a technical point of view, these methods can be categorized, as shown in Figures 1 and 2 [20]. Over the last decade, artificial intelligence techniques such as particle swarm optimization (PSO), neural networks (NNs), and the genetic algorithm have been utilized in temperature monitoring [20].

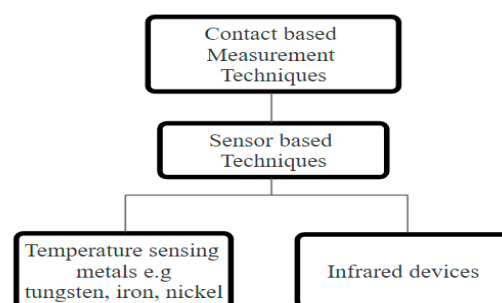


Figure 1. Categorization of stator temperature measurement methods.

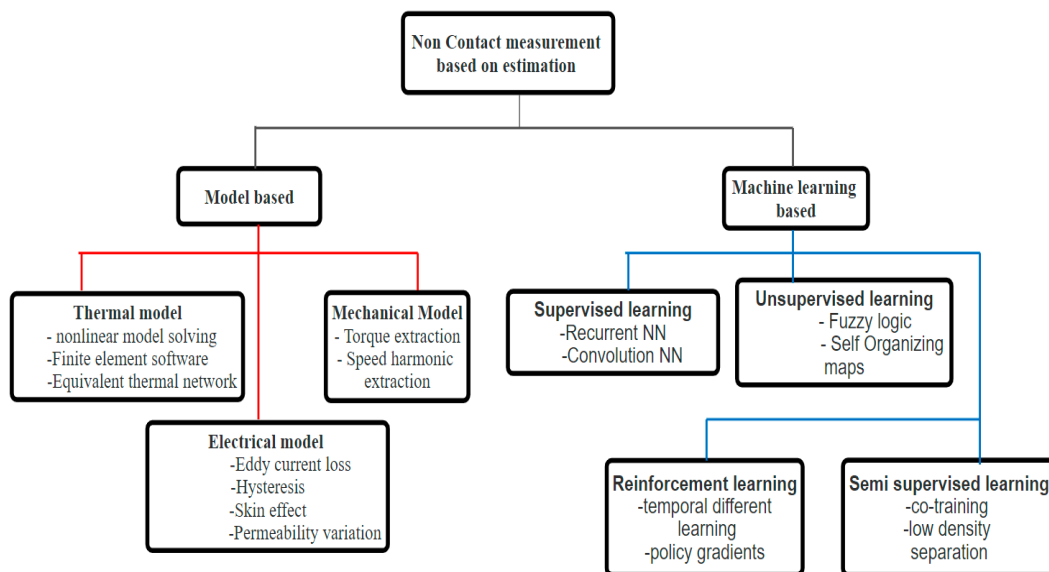


Figure 2. Estimation-based stator winding insulation temperature monitoring methods.

This paper uses historical data on stator winding temperatures to predict temperature behavior over time and, hence, provide information for preventive maintenance. Recently, artificial intelligence and machine learning-based techniques have attracted the attention of researchers in the assessment of insulation conditions since they are non-intrusive and easy to apply.

2.6. Prediction of Stator Winding Leakage Current

Insulation breakdown leads to the establishment of abnormal paths that encourage the flow of leakage currents. Thermal, electrical, environmental, and mechanical stresses on the insulation material will cause leakage current paths to develop within the winding insulation. The level of severity of the insulation deterioration is a perfect indicator of the magnitude of the leakage current flowing in the abnormal path. It is often difficult to precisely localize the source of the leakage current within the winding insulation.

The resultant leakage current is due to capacitive and resistive leakage currents, which is shown in Equation (6)

$$i_t = i_r + i_c \quad (6)$$

The capacitive leakage current, i_c , occurs as a result of alternating current flowing between conductors separated by a dielectric. Resistive leakage current, i_r , is a result of current loss via the insulation around the conductor. Resistive and capacitive leakage currents are dependent on the supply voltage. It is only the magnitude of the resistive leakage current that determines the integrity of the insulation material. Deterioration of the insulation resistance is escalated through rising values of the resistive leakage current. Additionally, the leakage current has a direct proportionality to surface contaminants on the insulator, that is, more leakage current flows with more contaminant deposits. For instance, water trappings under a layer of contaminants cause the insulation surface resistance to decrease. Therefore, Equation (7) shows that for an area S of a contaminant layer, then [21,22]:

$$S = \pi(r_2^2 - r_1^2) \quad (7)$$

where r_1 and r_2 are the insulator radius and the total radius of the contaminant layer and the insulator, respectively. Notably, a fault is not implied when the leakage current suddenly rises, followed by a decreasing steady trend over a short period of time. It can, however, imply that there has been a humidity increase around the insulators. Preventative maintenance should be performed if the leakage current values do not decrease with time.

Therefore, it is important to estimate the flow of these currents over time using historical data in order to assess the health of the insulation material. Monitoring of motor winding insulation can be performed by tracking physical properties such as the leakage current. Common techniques employed by researchers include wavelet transform, Fourier transform, and matched filters [23–25]. The drawbacks to these approaches include intensive computations, while wavelet and Fourier transforms are only efficient for steady-state diagnoses. Recently, several machine learning and artificial intelligence techniques have been developed for classification and prediction problems. For instance, neural networks, support vector machines (SVMs), K-nearest neighbors, and long short-term memory (LSTM) deep learning have gained popularity in anomaly detection. In [26], a support vector machine is applied in the classification of inter-turn leakage currents in the stator windings. The SVM frequency pattern is presented in [27] for leakage current fault detection in motor windings. However, SVM is limited by the careful need to precisely choose its parameters and those of the optimization algorithms. Neural networks are utilized in [28,29] for the detection of leakage current faults in stator windings. However, the neural network technique demands a large amount of data for training and testing. The deep learning classification of leakage currents between phases and phase-to-neutral is studied using LSTM in [30].

3. Methodology: Optimization of Random Forest Regression

The classical random forest algorithm structure is shown in Figure 3 [31]. Multiple prediction models were combined from several learning algorithms, i.e., decision trees, to achieve the most accurate prediction model. The mean from several trees was used as the overall output.

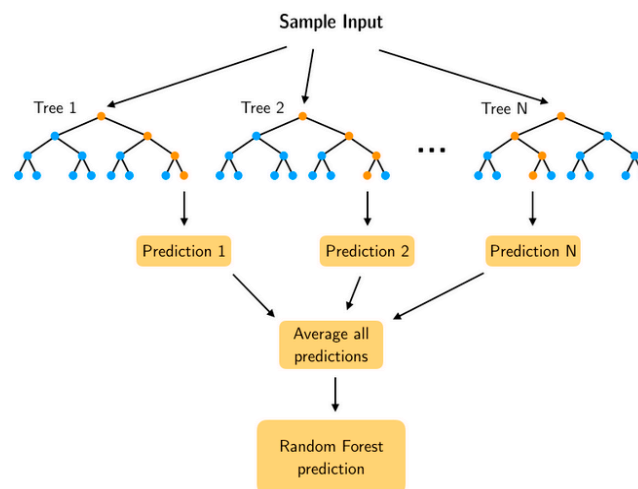


Figure 3. Conventional Random Forest regressor structure.

Bootstrap aggregating was used for training the tree learners in random forest. For $X = x_1, \dots, x_n$ as the training data set and $Y = y_1, \dots, y_n$ as responses, random samples with replacements were selected repeatedly K times from the training set. Trees were then fitted to the selected samples as follows.

For $k = 1, \dots, K$:

1. M Training examples are sampled with replacement from X_k and Y_k ;
2. A regression tree f_k is trained on X_k and Y_k ;
3. For all the predictions from different regression trees, the average is computed as follows:

$$\hat{f} = \frac{1}{K} \sum_{k=1}^K f_k(x')$$

where x' represents the unseen samples.

3.1. Hyperparameter Tuning in Random Forest Regression

The hyperparameters in the random forest algorithm include a number of decision trees ($n_estimators$), number of features ($max_features$) for node splitting, minimum number of samples ($min_samples_split$) that can cause node splitting, and maximum depth (max_depth) of an individual tree. The choice of these parameters depends on expert knowledge and may therefore be challenging to determine. Several algorithms have been proposed in the literature for hyperparameter tuning where a large number of parameters are presented to choose from. Some of the common hyperparameter tuning methods include the Bayesian approach [32], GridSearch [33], and RandomizedSearch [34]. GridSearch is commonly used in the literature as it is efficient in determining the best hyperparameters from a large search space as compared to RandomizedSearch. However, with an increased number of evaluations, the computation time also increases exponentially with the GridSearch algorithm.

Research results from [35–37] have shown that the genetic algorithm (GA) can be used to effectively optimize the random forest algorithm (RF). However, most of the GA optimization under study focuses on classification problems with categorical data.

The main contribution of this article involves RF optimization for estimation problem with continuous data. The stator winding temperature and leakage current data were obtained from a laboratory setup as in [30]. GA was used to intricately generate the best parameters, which were then used to fit the training data. A moving average function was then applied to the output to increase the accuracy of the prediction. The proposed process is shown in Figure 4. The performance of the proposed method was then compared with that of the feedforward neural network and long short-term memory algorithms using the same preprocessed data set.

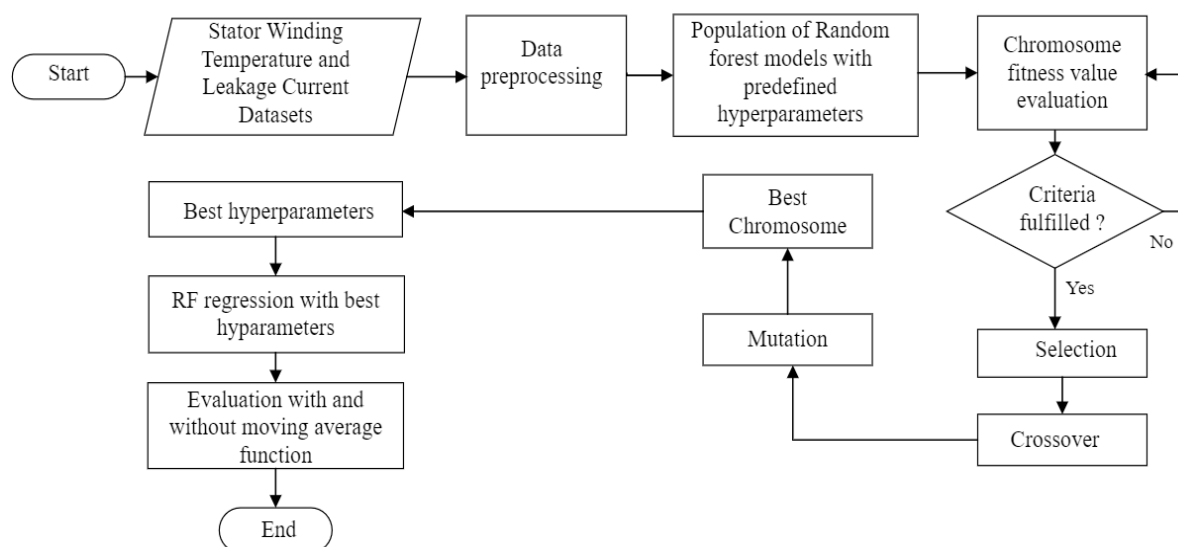


Figure 4. Proposed prediction model workflow.

Predefined values were initialized for the hyperparameters in N , the number of models. The accuracy of every model was determined, and only a fraction of the best-performing models was retained after an iteration. Offsprings similar to the selected hyperparameters were then generated for replacement back to the same number of models of the N population. A repeat cycle was performed for the given number of generations where only the best models survive when the process comes to an end.

3.2. Moving Average Filtering

Here, the next value of a variable, \hat{y} , of the data set is dependent on the average of the previous values k :

$$\hat{y} = \frac{1}{k} \sum_{m=1}^k y_{t-m} \quad (8)$$

Moving average window = 100 is implemented using the Python library bottleneck. A wider window was observed to present a smoother trend in the predicted output and to increase accuracy.

4. Results and Discussion

Since it is challenging to measure stator temperature, torque, and leakage currents in practical applications, a well-trained prediction model can be used to eliminate practical measurement devices. The effects of temperatures and leakage currents on insulation winding have been discussed in Section 1, and their trends can be utilized to inform on insulation integrity over time. In this paper, the performance of GA-based random forest regression, neural networks, and long short-term memory was compared in the time series forecasting of stator winding temperatures using historical data. The data used here for a demonstration of insulation health monitoring using physical quantities were acquired from a public data set presented by [30] from real laboratory experiments. The data were then preprocessed according to the requirements of the utilized estimation algorithm. Mean Absolute Error, Mean Square Error, and validation loss were used to validate the performance of the modeled algorithms.

4.1. Stator Winding Temperature Estimation with the Proposed Method

4.1.1. Estimation with Optimized Random Forest Regression

The data set was split into training and test data at 70% to 30%, respectively. GA was used to search for the best hyperparameters, which were then used for model fitting. Figure 5 shows the performance of the prediction model with the stator winding temperature as the target value for test run 51. The Mean Absolute Error (MAE) and Mean Squared Error (MAE) were calculated to gauge the performance of the model. In Figure 5, the black line plot represents the true value, while the red plot is the prediction plot.

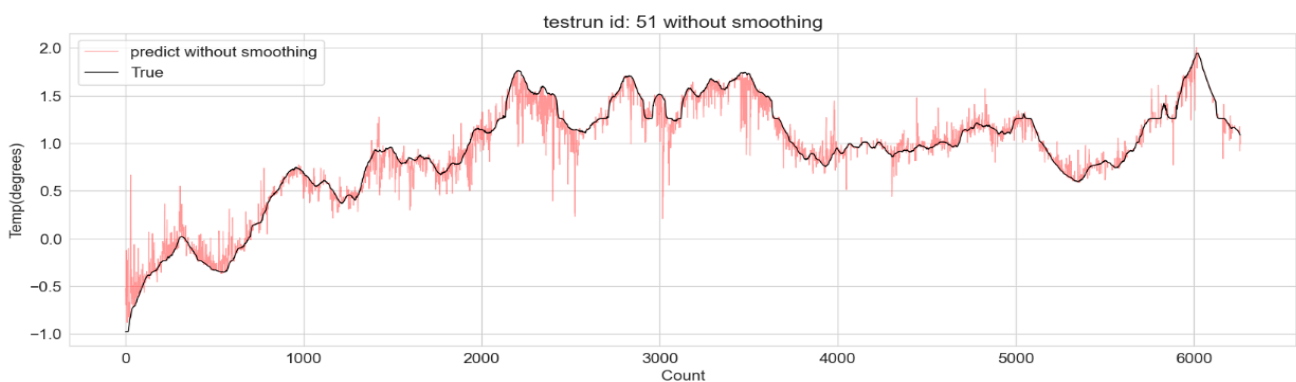


Figure 5. Tracking stator winding temperature data without moving average filter.

The moving average function not only filtered the noise, Figure 6, it also improved the MSE and MAE values. Metrics without moving average smoothing: MSE: 0.0163 and MAE: 0.0615, while Metrics with moving average smoothing: MSE: 0.0140 and MAE: 0.0505.

4.1.2. Estimation with Feedforward Neural Network

For 200 epochs and a batch size of 1000, a feedforward neural network was trained on the same data set as linear regression. Figure 7 shows the performance of the prediction model with the stator winding temperature as the target value for test run 51.

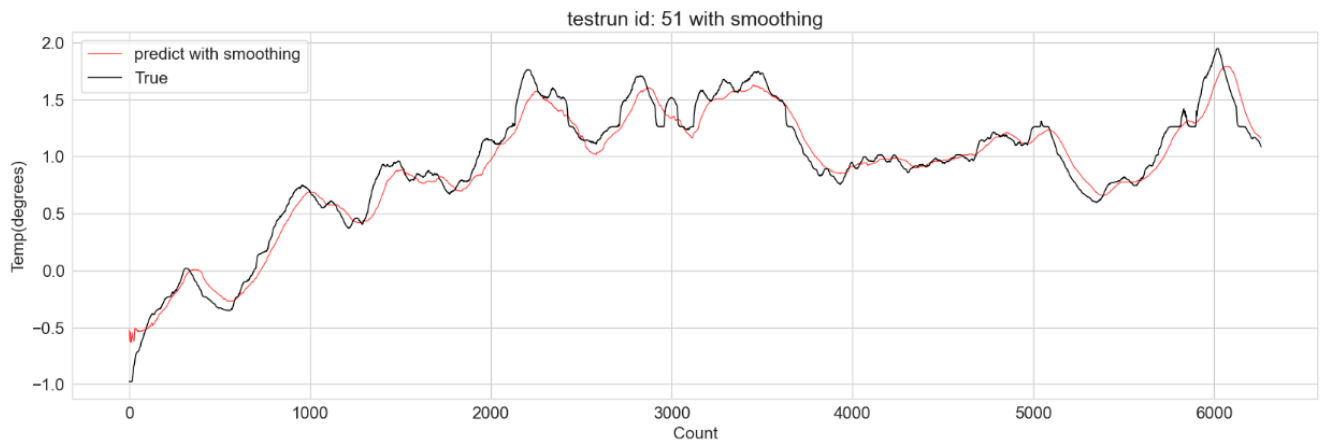


Figure 6. Prediction with GA-RF and moving average filter.

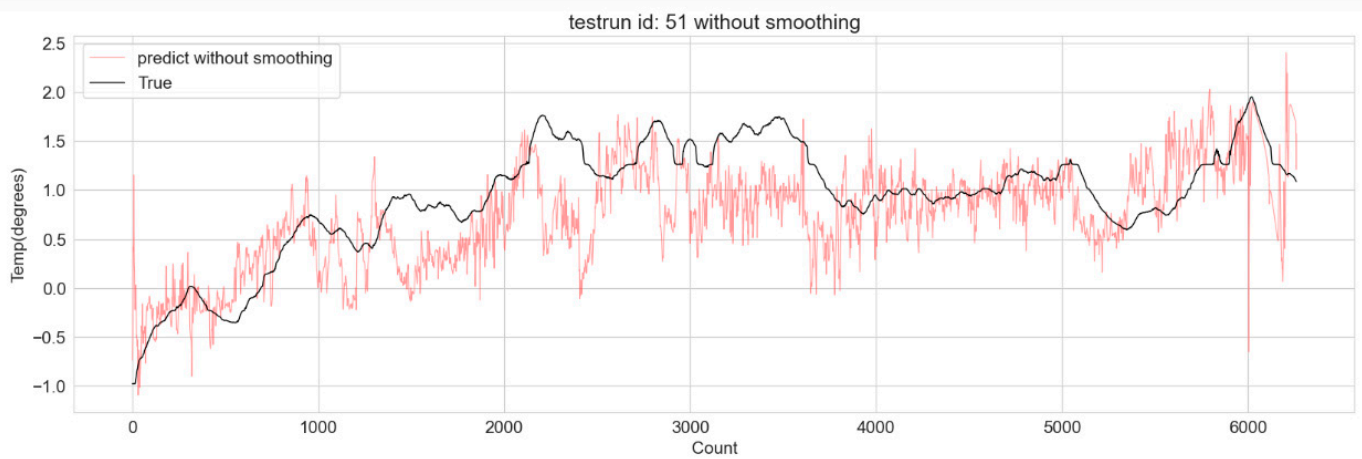


Figure 7. Tracking stator winding temperature with Feedforward neural network without moving average filter.

Figure 8 shows the performance of the prediction model for the stator winding temperature as the target value for test run 51 but with moving average function added to the GA-RF model.

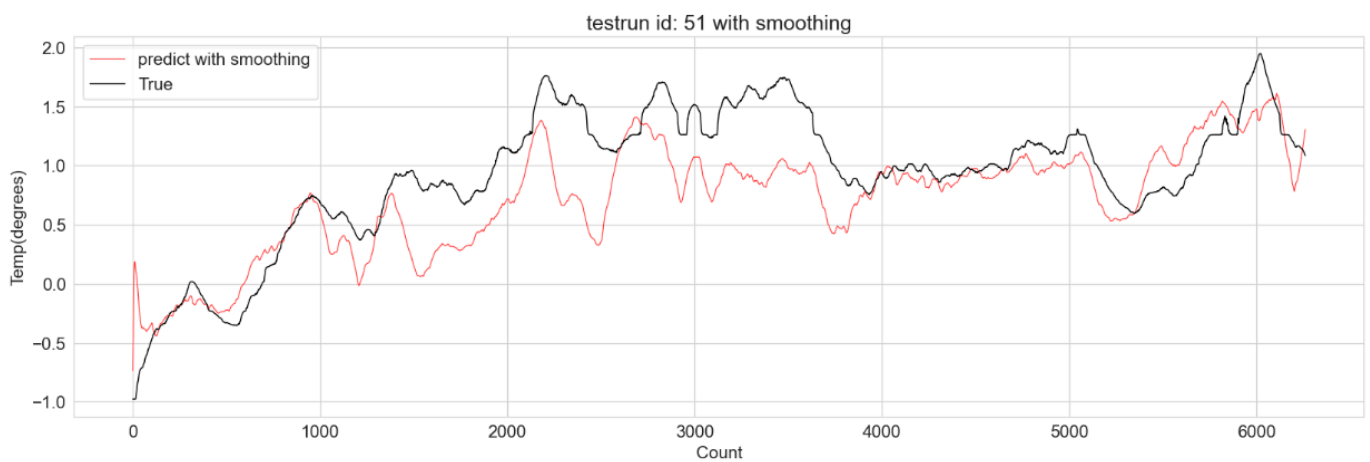


Figure 8. Tracking stator winding temperature with Feedforward neural network with moving average filter.

4.1.3. Estimation with Long Short-Term Memory (LSTM)

An LSTM model of window size = 100, sample rate = 10, epoch = 200, and batch size = 500 is used for Figure 9.

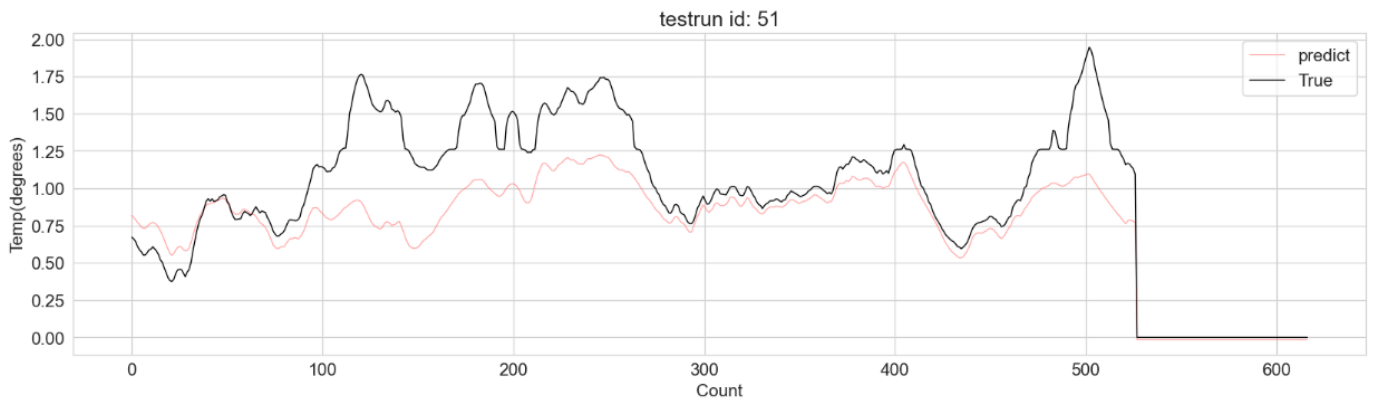


Figure 9. Stator Temperature behavior with LSTM.

4.1.4. Performance Evaluation

The MSE and MAE of the three prediction models are compared in Table 6.

Table 6. Performance metrics for different prediction models.

	GA-RF	Feedforward NN	LSTM
MSE	0.01403	0.14774	0.03696
MAE	0.05056	0.30563	0.16622

Table 6 shows that the proposed method has the lowest MSE and MAE values followed by LSTM. The optimized random forest regressor performs better than feedforward NN and LSTM in predicting stator winding temperature for the given data set. However, random forest regression plots are very noisy, especially where there is a lot of variation in the true data. Moreover, the GA-RF combination requires a lot of computation time and more powerful machine hardware. LSTM did not present any noise in its output; however, feedforward NN presents better model accuracy than LSTM, as shown in Table 7. The accuracy of the three models was determined using R-Squared Score with the values validating the better performance of the proposed algorithm.

Table 7. Comparison of model accuracy.

	GA-RF	Feedforward NN	LSTM
Accuracy	92.56%	87.45%	67.56%

The accuracy of each model calculated using the R-Squared Score is shown in Table 7. The validation loss and the training loss curves are depicted in Figures 10 and 11. The LSTM model is underfitting and therefore needs improvement. However, this is outside the scope of this study.

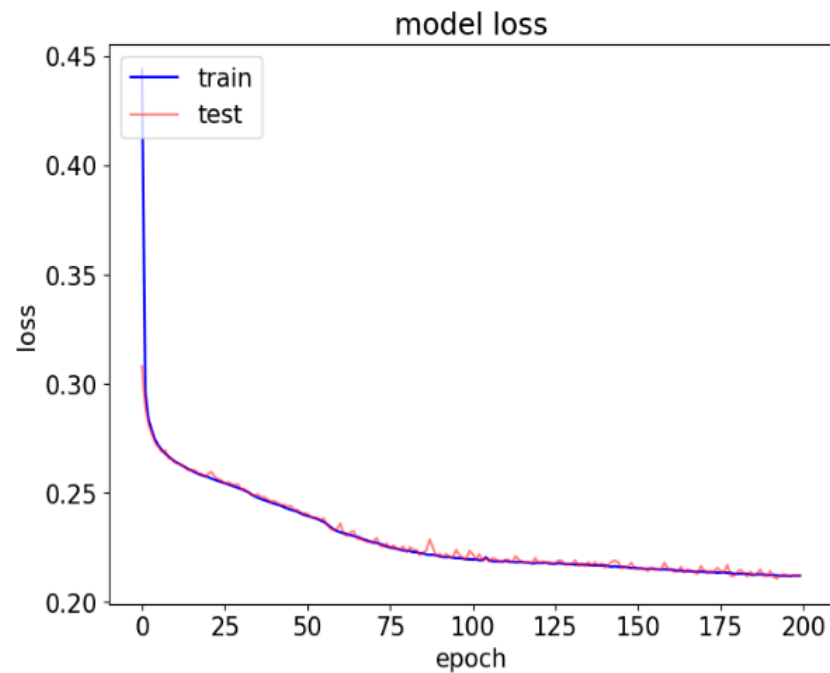


Figure 10. Feedforward NN training loss and validation loss.

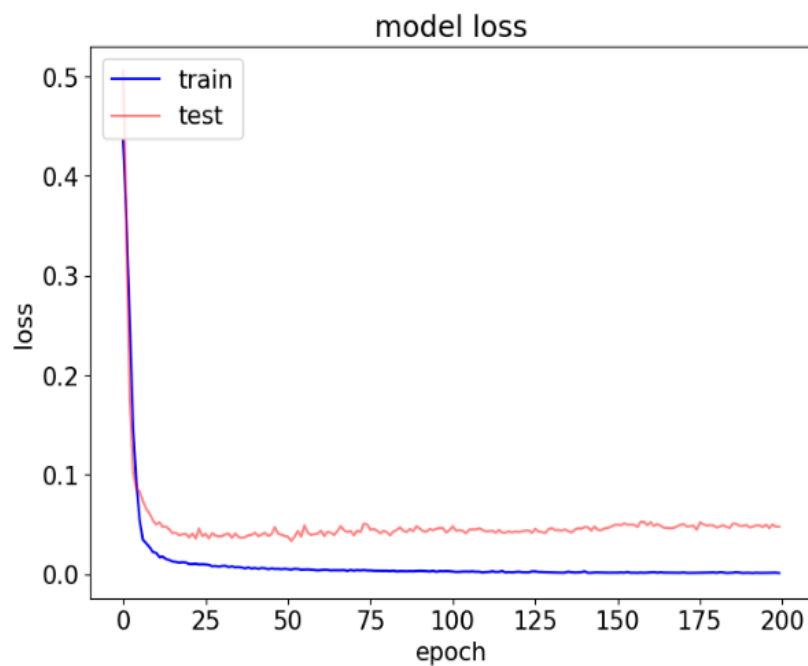


Figure 11. LSTM training loss and validation loss.

4.2. Leakage Current Estimation with the Proposed Method

Similarly, the effects of stator leakage currents on insulation winding have been discussed in Section 1. In this section, the performance of the GA-tuned random forest regression, feedforward NN, and LSTM was compared in the time series forecasting of stator leakage current using historical data. The data used here for a demonstration of insulation health monitoring using physical quantities were acquired from a public data set presented by [30] from laboratory experiments. The data were then preprocessed according to the requirements of the utilized estimation algorithm. Mean Absolute Error, Mean Square Error, and validation loss were used to validate the performance of the modeled algorithms.

4.2.1. Leakage Current Estimation with Optimized Random Forest Regression

Figure 12 represents the performance of the proposed model on estimation of leakage current. Moving average filter is introduced to improve the metrics as represented in Figure 13.

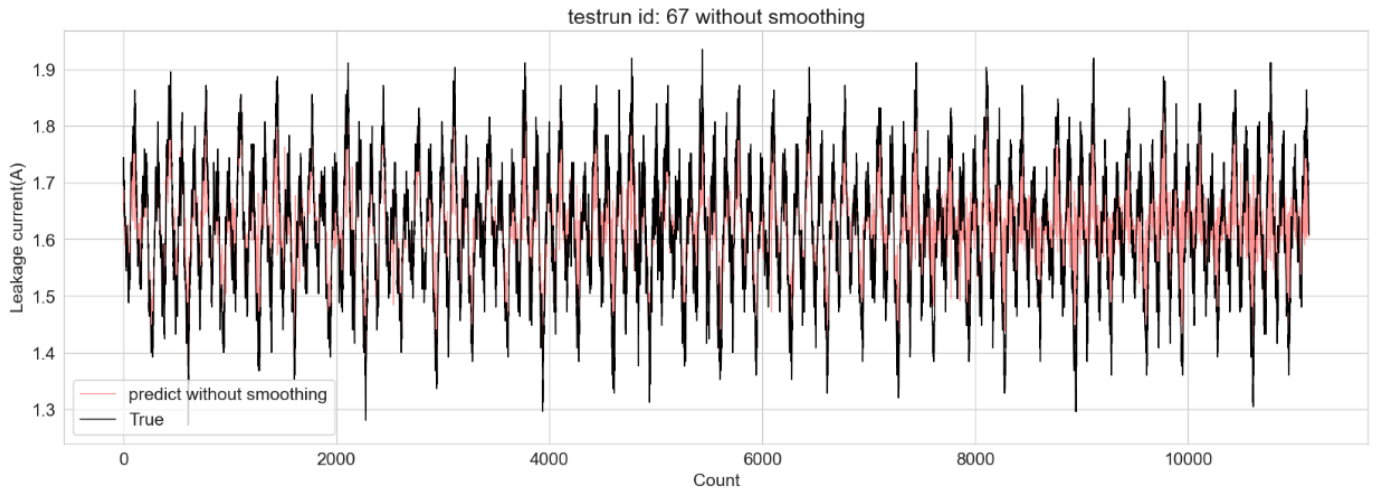


Figure 12. Leakage current prediction with GA-RF method.

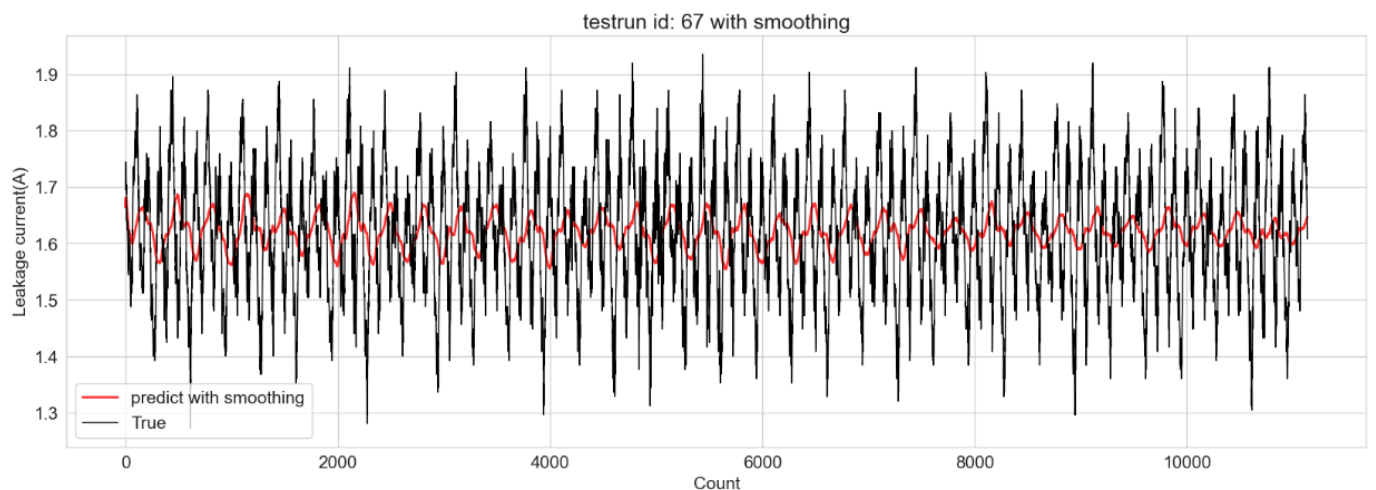


Figure 13. Leakage current prediction with GA-RF method and moving average filter.

4.2.2. Leakage Current Estimation with Feedforward Neural Network

Figures 14 and 15 shows the performance of the feed forward neural network model with three hidden layers. Introduction of moving average filter does not present noticeable improvement as shown in Figure 15.

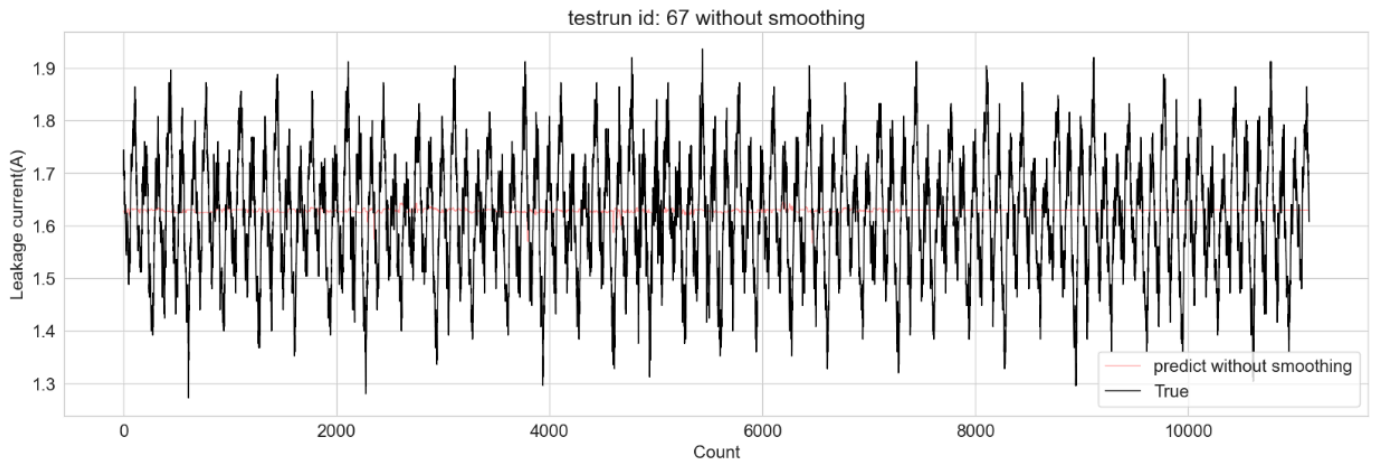


Figure 14. Leakage current prediction with Feedforward neural network.

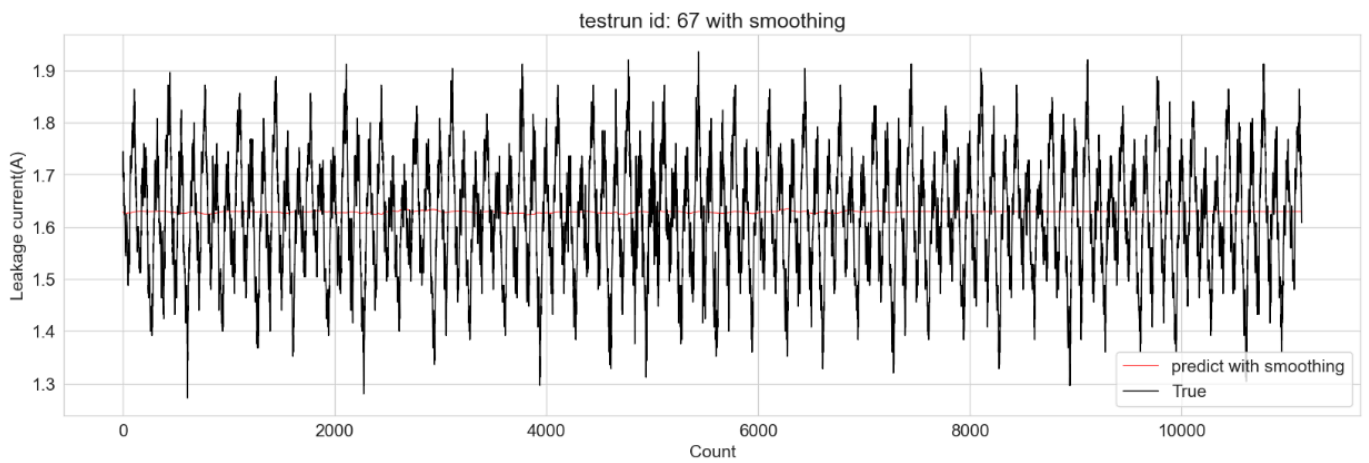


Figure 15. Leakage current prediction with Feedforward neural network combined with filtering.

4.2.3. Leakage Current Estimation with LSTM

Figure 16 shows the performance of the LSTM model in leakage current estimation. The LSTM model poor performance could be attributed to under fitting problem.

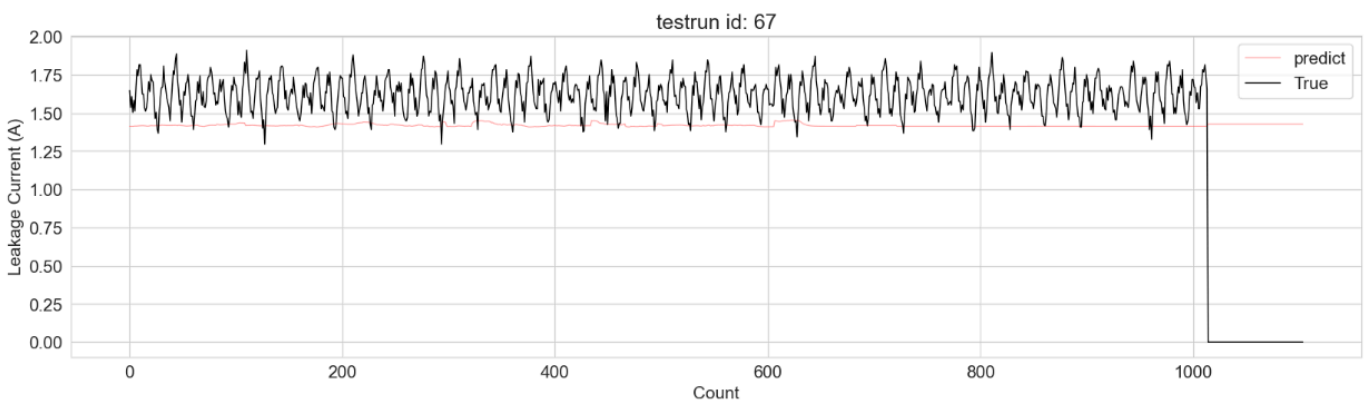


Figure 16. Leakage current prediction with LSTM.

4.2.4. Performance Evaluation in Leakage Current Estimation

The MSE and MAE of the three prediction models are compared in Table 6.

Table 8 shows that random forest performs better than feedforward NN and LSTM in predicting stator winding leakage current for the entire data set. The performance of

the models is also depicted in Figures 13, 14 and 16. Random forest regression is seen to perform better than the two algorithms. However, random forest regression plots are very noisy, especially where there is a lot of variation in the true data. The combination of GA and RF demands high computation power and also the computation time is very long. LSTM is less noisy compared to both NN and RF.

Table 8. Performance metrics for different prediction models for the entire data set.

	GA-RF	Feedforward NN	LSTM
MSE	0.005973	0.012353	0.16967
MAE	0.058421	0.091112	0.31292

5. Conclusions

The insulation integrity of SRM highly influences its efficiency and reliability. Two of the related factors that degrade the winding insulation are the stator winding temperature and the winding leakage current. Thermal modeling of SRMs is usually very complex since the precise calculation of core losses, as the cause of heat generation, is a difficult task. Additionally, insulation wires can be designed to withstand high-temperature operations, but this would introduce additional costs at the point of manufacture. With these in mind, this article has successfully investigated new methods of winding temperature and leakage current estimation and prediction to solve the complexity of thermal modeling and analysis. Moreover, these methods can also address the uncertainty of sensor faults. Early detection of anomalies in air temperature inside the motor and leakage currents can be used in planning for preventive maintenance of the winding insulations. Three prediction and estimation techniques were investigated, namely, random forest regression, feedforward neural networks, and long short-term memory. The optimized random forest regression performed better than the two techniques. However, the structure of LSTM can be improved to realize better performance at the expense of a larger computation memory.

Author Contributions: Conceptualization, L.S. and J.O.; methodology, J.O.; software, J.O.; formal analysis, J.O.; resources, L.S.; writing—original draft preparation, J.O.; writing—review and editing, L.S. and J.O.; supervision, L.S. All authors have read and agreed to the published version of the manuscript.

Funding: This research received no external funding.

Data Availability Statement: The data used were obtained from a public data set available at <https://www.sciencedirect.com/science/article/pii/S2666546823000460> (accessed on 12 February 2024).

Acknowledgments: The authors would like to thank the Department of Electric Power Engineering, Budapest University of Technology and Economics for the resources provided.

Conflicts of Interest: The authors declare no conflicts of interest.

References

- Hemmati, R.; Wu, F.; El-Refaie, A. Survey of Insulation Systems in Electrical Machines. In Proceedings of the 2019 IEEE International Electric Machines & Drives Conference (IEMDC), San Diego, CA, USA, 12–15 May 2019; pp. 2069–2076.
- Barré, O.; Napame, B. The Insulation for Machines Having a High Lifespan Expectancy, Design, Tests and Acceptance Criteria Issues. *Machines* **2017**, *5*, 7. [[CrossRef](#)]
- Danikas, M.G.; Karlis, A. A Review on Electrical Machines Insulation Aging and Its Relation to the Power Electronics Arrangements with Emphasis on Wind Turbine Generators. *Renew. Sustain. Energy Rev.* **2011**, *15*, 1748–1752. [[CrossRef](#)]
- Mayoux, C. Degradation of Insulating Materials under Electrical Stress. *IEEE Trans. Dielect. Electr. Insul.* **2000**, *7*, 590–601. [[CrossRef](#)]
- Florkowski, M.; Florkowska, B.; Zydron, P. Partial Discharges in Insulating Systems of Low Voltage Electric Motors Fed by Power Electronics—Twisted-Pair Samples Evaluation. *Energies* **2019**, *12*, 768. [[CrossRef](#)]
- Wood, J.W. Mechanical Stresses in Rotating Machines and Insulation Design Considerations. In Proceedings of the IEE Colloquium on the Mechanical Influence on Electrical Insulation Performance, London, UK, 28 February 1995; Volume 1995, p. 2.

7. Decner, A.; Baranski, M.; Jarek, T.; Berhausen, S. Methods of diagnosing the insulation of electric machines windings. *Energies* **2022**, *15*, 8465. [[CrossRef](#)]
8. Torkaman, H.; Karimi, F. Measurement Variations of Insulation Resistance/Polarization Index during Utilizing Time in HV Electrical Machines—A Survey. *Measurement* **2015**, *59*, 21–29. [[CrossRef](#)]
9. *IEEE Std 43-2000*; Recommended Practice for Testing Insulation Resistance of Rotating Machinery. IEEE: Piscataway, NJ, USA, 2000.
10. Gonzalez, E.A.; Petráš, I.; Ortigueira, M.D. Novel Polarization Index Evaluation Formula and Fractional-Order Dynamics in Electric Motor Insulation Resistance. *Fract. Calc. Appl. Anal.* **2018**, *21*, 613–627. [[CrossRef](#)]
11. Sabah, A.N.; Jaffery, Z.A. Fault detection of induction motor using thermal imaging. In Proceedings of the 2022 IEEE IAS Global Conference on Emerging Technologies, Arad, Romania, 20–22 May 2022. [[CrossRef](#)]
12. Tshiloz, K.; Smith, A.C.; Tuohy, P.M.; Feehally, T. Investigation of wire insulation for high-temperature motor windings. *J. Eng.* **2019**, *17*, 4442–4445. [[CrossRef](#)]
13. Roger, D.; Ait-Amar, S.; Napieralska, E. A method to reduce partial discharges in motor windings fed by PWM inverter. *Open Phys.* **2018**, *16*, 599–604. [[CrossRef](#)]
14. Reis, R.R.; Kimpara, M.L.; Pinto, J.O.; Fahimi, B. Multi-physics simulation of 6/4 switched reluctance motor by finite element method. *Eletrônica De Potência* **2021**, *26*, 8–18. [[CrossRef](#)]
15. Bilgin, B.; Jiang, J.W.; Emadi, A. *Switched Reluctance Motor Drives: Fundamentals to Applications*; CRC Press: Boca Raton, FL, USA, 2019.
16. Faiz, J.; Iranpour, R.; Pillay, P. Thermal Model for a Switched Reluctance Motor of TEFC During Steady-State and Transient Operation. *J. Electr. Mach. Power Syst.* **1998**, *26*, 77–92. [[CrossRef](#)]
17. Frosini, L. Novel diagnostic techniques for rotating electrical machines—A review. *Energies* **2020**, *13*, 5066. [[CrossRef](#)]
18. Burke, R.; Giedymin, A.; Wu, Z.; Chuan, H.; Bourne, N.; Hawley, J.G. A Lumped Parameter Thermal Model for Single-Sided AFPM Machines with Experimental Validation. *IEEE Trans. Transp. Electrification* **2020**, *6*, 1065–1083. [[CrossRef](#)]
19. Erazo, D.E.G.; Wallscheid, O.; Böcker, J. Improved Fusion of Permanent Magnet Temperature Estimation Techniques for Synchronous Motors Using a Kalman Filter. *IEEE Trans. Ind. Electron.* **2020**, *67*, 1708–1717. [[CrossRef](#)]
20. Meng, T.; Zhang, P. A review of thermal monitoring techniques for radial permanent magnet machines. *Machines* **2021**, *10*, 18. [[CrossRef](#)]
21. Amin, M.; Amin, S.; Ali, M. *Monitoring of Leakage Current for Composite Insulators and Electrical Devices [Online]*; University of Engineering and Technology: Taxila, Pakistan, 2007; Available online: http://phys.mech.nw.ru/e-journals/RAMS/no_12109/amin.pdf (accessed on 28 January 2018).
22. Davis, D. Real vs. Total Current Achiptot Testing Determines True Insulation Quality [Online]. Lake Bluff, IL, USA. Available online: <http://www.pema.ie/TECHTALK%20LIBRARY/Associated%20Research/ARept.pdf> (accessed on 7 October 2023).
23. Ebrahimi, B.M.; Faiz, J.; Roshtkhari, M.J. Static-, dynamic-, and mixed eccentricity fault diagnoses in permanent-magnet synchronous motors. *IEEE Trans. Ind. Electron.* **2009**, *56*, 4727–4739. [[CrossRef](#)]
24. Choi, S.-D.; Akin, B.; Kwak, S.; Toliyat, H.A. A compact error management algorithm to minimize false-alarm rate of motor/generator faults in (hybrid) electric vehicles. *IEEE J. Emerg. Sel. Top. Power Electron.* **2014**, *2*, 618–626. [[CrossRef](#)]
25. Khan, M.A.S.; Rahman, M.A. Development and implementation of a novel fault diagnostic and protection technique for IPM motor drives. *IEEE Trans. Ind. Electron.* **2008**, *56*, 85–92. [[CrossRef](#)]
26. Pietrzak, P.; Wolkiewicz, M. Application of support vector machine to stator winding fault detection and classification of permanent magnet synchronous motor. In Proceedings of the 2021 IEEE 19th International Power Electronics and Motion Control Conference (PEMC), Gliwice, Poland, 25–29 April 2021; pp. 880–887.
27. Ebrahimi, B.M.; Faiz, J. Feature extraction for short-circuit fault detection in permanent-magnet synchronous motors using stator-current monitoring. *IEEE Trans. Power Electron.* **2010**, *25*, 2673–2682. [[CrossRef](#)]
28. Quiroga, J.; Cartes, D.; Edrington, C.; Liu, L. Neural network based fault detection of PMSM stator winding short under load fluctuation. In Proceedings of the 2008 13th International Power Electronics and Motion Control Conference, Poznan, Poland, 1–3 September 2008; pp. 793–798.
29. Nyanteh, Y.; Edrington, C.; Srivastava, S.; Cartes, D. Application of artificial intelligence to real-time fault detection in permanent-magnet synchronous machines. *IEEE Trans. Ind. Appl.* **2013**, *49*, 1205–1214. [[CrossRef](#)]
30. Sun, Z.; Machlev, R.; Wang, Q.; Belikov, J.; Levron, Y.; Baimel, D. A public data-set for synchronous motor electrical faults diagnosis with CNN and LSTM reference classifiers. *Energy AI* **2023**, *14*, 100274. [[CrossRef](#)]
31. Al-Gabalawy, M.; Elmetwaly, A.H.; Younis, R.A.; Omar, A.I. Temperature prediction for electric vehicles of permanent magnet synchronous motor using robust machine learning tools. *J. Ambient. Intell. Humaniz. Comput.* **2022**, *15*, 243–260. [[CrossRef](#)]
32. Gauffin, C. Rotor Temperature Estimation in Induction Motors with Supervised Machine Learning. Master’s Thesis, KTH Royal Institute of Technology, Stockholm, Sweden, 2023. Available online: <http://kth.diva-portal.org/smash/get/diva2:1805112/FULLTEXT01.pdf> (accessed on 8 March 2024).
33. Sixto, A. Electric Motor Temperature Estimation Using Regression Models. *Medium*. 2020. Available online: <https://medium.com/@abisixto/electric-motor-temperature-estimation-using-regression-models-9200697746e1> (accessed on 9 March 2024).

34. Koehrsen, W. Hyperparameter Tuning the Random Forest in Python. *Medium*. 10 January 2018. Available online: <https://towardsdatascience.com/hyperparameter-tuning-the-random-forest-in-python-using-scikit-learn-28d2aa77dd74> (accessed on 27 February 2024).
35. Ansari, S. Hyperparameter Tuning in Random Forest Classifier Using Genetic Algorithm. *Medium*. 10 October 2020. Available online: <https://sakilansari4.medium.com/hyperparameter-tuning-in-random-forest-classifier-using-genetic-algorithm-ae582ae6655c> (accessed on 9 March 2024).
36. Yang, L.; Shami, A. On hyperparameter optimization of machine learning algorithms: Theory and practice. *Neurocomputing* **2020**, *415*, 295–316. [[CrossRef](#)]
37. Elyan, E.; Gaber, M.M. A genetic algorithm approach to optimising random forests applied to class engineered data. *Inf. Sci.* **2017**, *384*, 220–234. [[CrossRef](#)]

Disclaimer/Publisher’s Note: The statements, opinions and data contained in all publications are solely those of the individual author(s) and contributor(s) and not of MDPI and/or the editor(s). MDPI and/or the editor(s) disclaim responsibility for any injury to people or property resulting from any ideas, methods, instructions or products referred to in the content.